

DESIGNING AND EVALUATING A PORTABLE LIDAR-BASED SLAM SYSTEM

P. Trybała^{1,2}, P. Kujawa¹, K. Romańczukiewicz¹, A. Szrek¹, F. Remondino²

¹ Faculty of Geoen지니어ing, Mining and Geology, Wrocław University of Science and Technology, Na Grobli 15, 50-421 Wrocław, Poland - Email: (pawel.trybala, paulina.kujawa, kinga.romanczukiewicz, aleksandra.szrek)@pwr.edu.pl

² 3D Optical Metrology (3DOM) unit, Bruno Kessler Foundation (FBK), Trento, Italy – Email: (ptrybala, remondino)@fbk.eu

ABSTRACT

Mobile Mapping Technology (MMT) has evolved rapidly over the past few decades, especially in using low-cost sensors. This progress is primarily attributed to the appearance of innovative simultaneous localization and mapping (SLAM) algorithms. This article focuses on evaluating the efficiency of a new LiDAR-based portable SLAM system for mapping in dynamic real-world environments. The work proposed a technical solution based on a Livox Avia LiDAR sensor enhanced by gimbal stabilization. The system, named Portable Livox-based Mapping system (PoLiMap), is compared to other similar solutions by acquiring data from various environments, including urban sceneries, underground tunnels and forested areas, and processing them using a modified FAST-LIO-SLAM algorithm. The research presented in the article contributes to the understanding of the capabilities of PoLiMap systems under various conditions and offers significant insight into its potential applications. Accuracy evaluation results prove that the proposed MMT system can successfully tackle various demanding environments and challenge the results of other more costly state-of-the-art portable mobile laser scanning methods.

KEY WORDS: Mobile Mapping, 3D reconstruction, Evaluation, Low-Cost, Urban mapping, Forest mapping, Cultural heritage.

1. INTRODUCTION

Advances in currently available technologies have greatly simplified the process of terrestrial 3D mapping in various conditions. However, different factors present in multiple environments, including dynamic objects, limited GNSS coverage, underground passages, reflective surfaces, dense and ever-changing vegetation, varying exposure to sunlight and more, pose a great challenge for developing a universal mobile mapping solution (Ali et al., 2020; Cheng et al., 2022). Achieving efficient 3D data collection and accurate reconstruction is possible with the use of Mobile Mapping Technologies (MMT) Systems. These devices equipped with different sensors, such as LiDARs (Elhashash et al., 2022; Ismail et al., 2022), radars (Rouveure et al., 2021; Glira et al., 2022) or cameras (Kolhatkar and Wagle, 2020; Torresani et al., 2021), enable the generation of precise and dense point clouds providing information about the geometric characteristics of the investigated area. The software backbone of MMTs is a Simultaneous Localization And Mapping (SLAM) method, either based on image or range data. SLAM allows to construct a map of the unknown environment while simultaneously estimating the sensor pose, and thus its trajectory during movement (Debeunne and Vivet, 2020). MMT sensors can be mounted on an autonomous robot (Wang et al., 2018), placed aboard a ground vehicle (Singandhupe and La, 2019) or UAV (Sonugür, 2023), but can also be used as a handheld device (Torresani et al., 2021).

The principle of the currently prevailing pose graph approach to solving the SLAM problem can be split into two main components: LiDAR or visual odometry and graph optimization. The former is responsible for continuous association of the data collected by the sensors at subsequent frames, either through direct methods, or using feature extraction and matching for estimating the relative change of the sensor pose in the analyzed period. Those estimates constitute the main factor in the pose graph, which together with other available data, can be useful for calculating the sensor motion (inertial measurements, GNSS observations, landmark positions) is optimized in the backend to produce the final, adjusted sensor trajectory results and thus, allowing accumulating all measurements in a coherent, global

map (He et al., 2022). In this study, one of the open-source LiDAR-based SLAM frameworks, FAST-LIO-SLAM (Kim et al., 2022a), is revisited, with the focus on improving its accuracy and robustness.

The need of developing such solution is to ensure user-friendly acquisitions and quality mapping results in challenging conditions, such as those of irregular, underground tunnels. This lies in the EIT-RM projects VOT3D - Ventilation Optimizing Technology based on 3D-scanning VOT3D which aims to reform the current ventilation design approach by incorporating accurate and detailed 3D surveying and modeling of airways (Figure 1) in airflow simulations. The introduction of modern methods and innovative solutions for underground optimisation in mining scenarios based on 3D data is crucial for the resources sector. The utilization of MMT in underground environments, despite being a challenge, is a key factor enabling realistic simulations of the ventilation system's operation within an industrial underground mine (Janus and Ostrogórski, 2022; Wróblewski et al., 2023). An understanding of the limitations and achievable quality standards associated with 3D data surveys performed in such peculiar environment is therefore important to guarantee the reliability of the entire optimisation process.

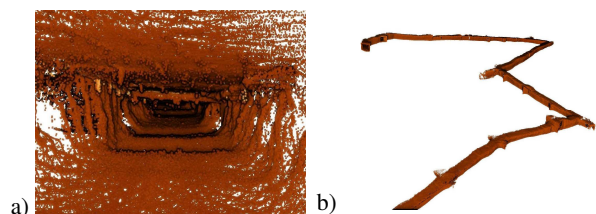


Figure 1. One of the underground test sites of the VOT3D project, surveyed with the proposed MMT system: view from inside the tunnel (a) and side view of the mining tunnel (b).

1.1 Paper aims

In the past, various SLAM systems and algorithms have been tested for 3D reconstruction of cultural heritage objects (Di

Stefano et al., 2021; Perfetti and Fassi, 2022), mapping of underground and underwater scenario (Farella, 2016; Menna et al., 2023; Trybała et al., 2023a), or natural environments such as forests (Qian et al., 2016; Hyyppä et al., 2020). However, a rapid progress in the developments in both hardware and software in MMTs has democratized the use of low-cost, reliable and increasingly accurate in-house-built SLAM-based systems. Thus, the aim of this paper is multi-folds:

- (i) to assemble a 3D surveying measurement system based on a Livox Avia LiDAR sensor stabilized with a gimbal and designed to be easily carried by an operator or placed on a vehicle;
- (ii) to couple the proposed handheld system, based on a solid-state LiDAR, with a state-of-the-art pose graph SLAM approach for real-time 3D mapping;
- (iii) to perform a metrological assessment of the proposed low-cost, lightweight MMT system in different environments (urban space, underground tunnel and forestry), using accurate ground truth data;
- (iv) to compare the proposed MMT system with other available mobile mapping solutions (GeoSLAM mobile scanner, multi-camera in-house photogrammetric system).

Data acquired with the proposed setup with and without the laser scanner mounted on a gimbal were also compared. The quality of both IMU signals and resulting point clouds were analyzed with the goal of assessing the extent to which external stabilization of the scanner improves data quality and reduces motion artefacts.

2. RELATED WORKS

Methods for acquiring 3D point clouds and assessing their accuracy to ensure their suitability for further analysis has been discussed repeatedly in the literature (Di Stefano et al., 2021; Tanduo et al., 2022; Trybała et al., 2023). The development of reality-based 3D surveying instruments and methods, and in particular MMT, has represented a significant progress in data acquisition in various environments. Application of MMT using SLAM algorithms in a complex urban environment was presented in Wang et al. (2018). In its review Mobile Laser Scanning (MLS) solutions, GNSS, IMU and applications are presented. Similarly, examination was carried out in the historic part of the urban centre of Venice by Tanduo et al. (2022), involving selected SLAM solutions, using a commercial backpack-mounted system and a handheld scanner. This assessment involved a comparative analysis of point clouds against TLS-derived ground truth data.

The use of a TLS and SLAM-based method in forest area mapping is described in Bienert et al. (2018) whereas Pan et al. (2023), present a system that integrates a dual laser scanners and an IMU system. Similar comparisons and combinations of SLAM-based methodologies with TLS data in forest areas are presented in Pierzchała et al. (2018), and Shao et al. (2020).

Nocerino et al. (2017) evaluated portable MMT in indoor and outdoor scenarios. Comparative analyses of point clouds acquired using commercial LiDAR-based SLAM algorithms and portable, mobile scanning devices are presented in Sesmero et al. (2021), Fasiolo et al. (2023), Trybała et al. (2023a).

Prados Sesmero et al. (2021) introduced an algorithm of graph SLAM applied in diverse environments, with particular emphasis on narrow, longitudinal facilities, especially tunnels, in which missing features and the problematic separation of different positions in the environment create difficulties to answer. Indoor and outdoor mapping studies on the performances of different SLAM algorithms in 3D mapping is presented in Akpınar (2021).

3. PROPOSED SYSTEM

The Portable Livox-based Mapping (PoLiMap) system was designed for convenient mobility during surveying operations. The LiDAR Livox Avia sensor (Table 1) is placed on a gimbal to ensure smooth motion and a secured grip, even when the sensor is used on a high speed vehicle (car, motorcycle). A NVIDIA Jetson Xavier board running Robot Operating System (ROS) as well as the rest of the necessary equipment (power supplies, Livox Converter 2.0, external drive and screen tablet) are placed in a suitcase (Figure 2).

Laser wavelength	905 nm	
Max. detection range (@ 100 klx)	From 190 m @ 10% reflectivity to 320 m @ 80% reflectivity	
Range precision	2 cm @ 100 m	
Angular precision	0.05°	
Scanning rate	10 Hz	
Scanning pattern	Line	Circular
Scanning mode	Repetitive	Non-repetitive
Field of view (horizontal x vertical)	70.4° x 4.5°	70.4° x 77.2°
Point rate	From 240,000 points/s to 720,000 points/s (triple return)	
Beam divergence	horizontal: 0.03° vertical: 0.28°	
Data Latency	≤ 2 ms	
Weight	0.5 kg	

Table 1. Livox Avia specification (Livox Avia Quick Start Guide v1.4, 2021).



Figure 2. Assembled PoLiMap and its equipment.

For processing the LiDAR data, the system runs a FAST-LIO LiDAR odometry (Kim et al., 2022a): it estimates the change in sensor pose based on inertial measurements coupled with subsequent point cloud matching with a point-to-plane iterative closest point (ICP) algorithm in a frame-to-local map manner. Moreover, it utilizes Scan Context++ (Kim et al., 2022b) as a loop closure detector and GTSAM-based pose graph optimization (Dellaert et al., 2022).

Due to past critical evaluations of SLAM frameworks (Trybała et al., 2023a) and other internal tests, several improvements have been implemented in FAST-LIO-SLAM librar:

- loop closure improvement: in the original implementation (Kim et al., 2022a), authors assumed constant, a priori assigned covariance values of each constraint in the pose graph. We used real covariance estimates for each measurement component, resulting from point cloud registration results in LiDAR odometry and fast generalized ICP-based (Koide, 2021) loop closures.
- loop candidate identification: we allow using intensity-based Scan Context++ (Kim et al., 2022b) instead of height-based default version to tackle scenarios with huge variations of LiDAR scanner orientation, such as handheld mapping of narrow spaces. Moreover relaxed parameter values for accepting a candidate loop detection to make Scan Context++ act as a quick heuristic of finding several reasonable candidates.
- rigorous loop closure verification: first the point clouds around both the historic and previous pose are aggregated in their neighbourhoods using current trajectory estimates and then downsampled with a rough-resolution voxel filter. The alignment is performed using fast voxelized generalized ICP (FastVGICP; Koide, 2021), assuming only a partial overlap between matched point clouds. It allows to reject in real-time multiple incorrect loop closures and provide a good initial guess for the precise registration, which is performed using FastGICP at much finer resolution if the matching error threshold is passed. Pre-aligning the point clouds facilitates achieving final convergence of the algorithm and speeds up the process.
- alternative metric computation: the registration error is usually computed as the root mean square error (RMSE) of the entire aligned point clouds. In our approach we limit the set of points included in the RMSE calculation to the same predefined overlap ratio used for registration or use percentile Hausdorff distance of a corresponding ratio.

Finally, a final check is performed if the loop candidate passes those tests. A hypothetical loop constrain is temporarily added to the pose graph. After optimizing the graph, adjustment error is computed, and if adding the loop causes a severe graph deformation, the hypothesis is rejected. This acts as an additional sanity check and reduces the number of incorrectly detected loops in distant areas similar to each other, which is a risk, e.g., in simple indoor environments.

All these changes aim to achieve centimeter-level loop closure and 3D mapping accuracy even in cases of very different sensor orientations and partial point cloud overlap, while still maintaining a reasonable speed of computations.

Although the implemented changes can add a noticeable overhead to the computation time, the results are obtained in close to real-time and the surveying process is not disturbed. In the worst case of loop closure detection and verification or pose graph optimisation taking too much time, LiDAR odometry with the resulting non-optimized point cloud is still performed in real-time thanks to the original multi-threaded implementation of the framework. This trade-off however allows to obtain more accurate results of 3D mapping through increasing robustness of utilizing loops in the pose graph, as well as improving its accuracy through multi-resolution point cloud registration. Finally, multiple variables, such as selection of a robust kernel for each type of pose graph constraint and variables of abovementioned new elements of the framework, have been additionally exposed as ROS parameters, allowing its easier adaptation to challenging mapping conditions.

4. EVALUATION

4.1 Test scenarios

To exhaustively evaluate the performances of the assembled 3D surveying system, different scenarios are chosen:

- a part of the campus of Wrocław University of Science and Technology (WUST) in Poland: the scene is particularly interesting because of its buildings of various sizes, geometries, surface types (concrete, glass, etc.) and architectural styles. The scene belongs to the MIN3D dataset (Trybała et al., 2023b):
- a single deciduous tree from the forest area representing the types of tall trees (height of approx. 17 m).
- a tight up-hill underground tunnel (“100 Scalini”), part of a large World War I fortification structure located in Mount Celva, Trento (Italy). The site structure is similar to that found in caves or historical mining areas.
- a small forest area composed of different types of trees and representing a natural environmental scene with varied and irregular geometry.

Additionally, a part of a tree-lined cobblestone street in an urban area was used to perform an ablation study of the proposed PoLiMap system (Section 5.1). The use case was selected for comparison of the system with and without the use of a gimbal to assess the impact of its use in scenarios of mapping environments with heavy vibrations.

4.2 Quality assessment methodology

To evaluate the quality of the data acquired with the proposed 3D surveying system, the SLAM-based points clouds were compared with ground truth (GT) data obtained using terrestrial laser scanning (TLS) or photogrammetry. The summarized scenarios with GT are included in Table 2.

For the campus WUST and single tree case studies, the GT point cloud was acquired with a RIEGL VZ-400i pulse TLS. The manufacturer’s declared accuracy of a single point is 5 mm, and the precision is 3 mm. Data processing including scan cloud cleaning, filtering, registration, and adjustment was performed in specialized RiSCAN PRO software.

For the other underground study area, GT data were acquired using a Leica BLK2GO mobile scanner. Additionally, the results were compared to two other point clouds, generated by a GeoSLAM ZEB Horizon and with a portable multi-camera photogrammetric system (Perfetti et al., 2022).

For the quantitative assessment of the produced 3D data, registered with the method proposed in Section 3, the Multiscale Model-to-Model Cloud Comparison (M3C2) method (Lague et al., 2013) against the GT point cloud was used and statistics were calculated to determine mapping error values. Accuracy and completeness analysis was also carried out (Knapitsch et al., 2017; Trybała et al., 2023a).

Scenario	Approx. size	Reference data
Outdoor university campus	60 x 20 m, 15 m height	RIEGL VZ-400i
Single tree	17 m height, 10 m (crown), 0.5 m (trunk) diameter	RIEGL VZ-400i
WWI tunnel	50 m length	BLK2GO, Zeb Horizon, photogrammetry
Forest area	60 x 40 m, 20 m height	BLK2GO

Table 2. Summarized case studies with reference data.

5. RESULTS

3D visualizations of the resulting point clouds along with close-ups are shown in Figure 3. The point clouds represent three different environments: urban, underground and natural. Urban environments include dense open spaces with complicated geometry of buildings and urban infrastructure, interspersed with natural elements such as trees, shrubs and plants. Acquiring 3D data for the uppermost parts of high buildings can be a challenge due to the scanner's limited range. In contrast, closed spaces, of which an underground tunnel is an example, do not cause such issues, but the data may be degraded or sparse due to multiple occlusions or lack of geometrical features. The last scenario, represented by a forest, is one of the most difficult environments for 3D reconstruction due to the scattering of points caused by leaves or branches. The resulting point cloud is non-uniform with increased level of random noise in the tree crowns.

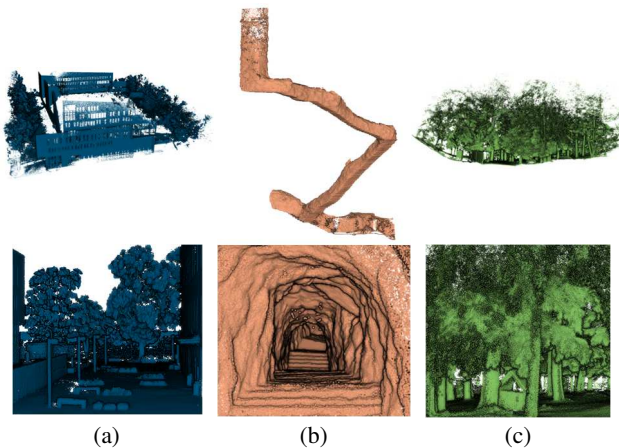


Figure 3. Visual impressions of the point clouds obtained with the proposed 3D surveying system: a fragment of the WUST campus (a), “100 Scalini” cultural heritage site (b) and the foresty area (c).

Figures 4 – 7 present the 3D reconstructions of selected objects acquired with the proposed portable PoLiMap system and their comparison to reference data. Statistics from those comparisons are compiled in Table 3.

For the WUST scenario, an analysis of specific man-made elements, including two building facades and a concrete substrate, reveals the smallest error on the ground level and a relatively larger error on the farther one of the building walls, partially obstructed by a fence. However, 95% of point were within 7 cm distance to the reference point cloud (Figure 4-top). For the tree object, due to occlusions and natural instability, tree foliage contains a lot of noise. The smallest deviations are observed on the outer parts of the crown the trunk, where standard deviation of M3C2 distances reaches 5.5 cm (Figure 4 – ceter ad bottom). Noteworthy to say that the general shape of the tree with its crown can still be distinguished.

For both cases, it can be noticed that the point cloud generated from the PoLiMap system shows a lower point density (approx. 800 points/m² for WUST campus and 700 points/m² for single tree) compared to the data collected with TLS (6600 points/m² and 1500 points per m², respectively).

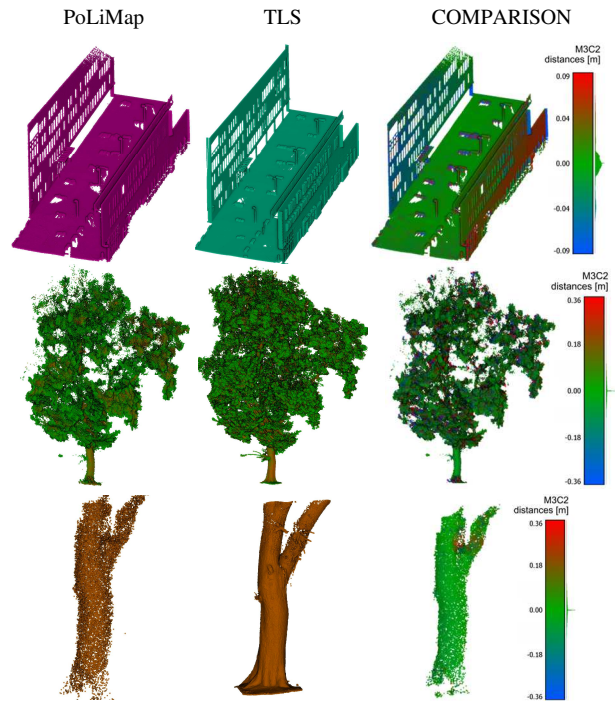


Figure 4. M3C2 comparison of point clouds from PoLiMap and TLS: a part of the WUST campus (top) and a single tree of the forest areas (center and bottom).

For the underground case, data obtained from the PoLiMap system, GeoSLAM and multi-camera photogrammetric solutions were benchmarked against data obtained from Leica BLK2GO mobile scanner. The Leica handheld solution offers a high measurement rate of 420,000 points per second, with a range noise of +/-3 mm and an indoor accuracy of +/-10 mm. Comparison with reference data showed very comparable mapping results of GeoSLAM and Livox. Both of them achieved standard deviations in the M3C2 comparisons (Figure 6) below 4 cm. The photogrammetric solution, although maintaining a correct shape of the tunnel, generated a slightly more noisy point cloud with the trajectory affected by a drift error. The errors were mostly accumulated in the vertical shaft at the end of the tunnel, which due to the constrained space could be captured from very limited perspectives, creating short baselines for the 3D reconstruction. As indicated in Table 3, excluding this part of the tunnel leads to achieving median error at level in line with other tested solutions. For all systems, the biggest differences, amounting to several centimeters, are noticeable at the inlet and outlet of the tunnel.

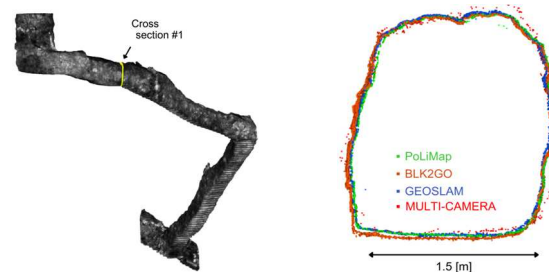


Figure 5. Visualization of the reference point cloud from “100 Scalini” (left) and the compared cross sections (right).

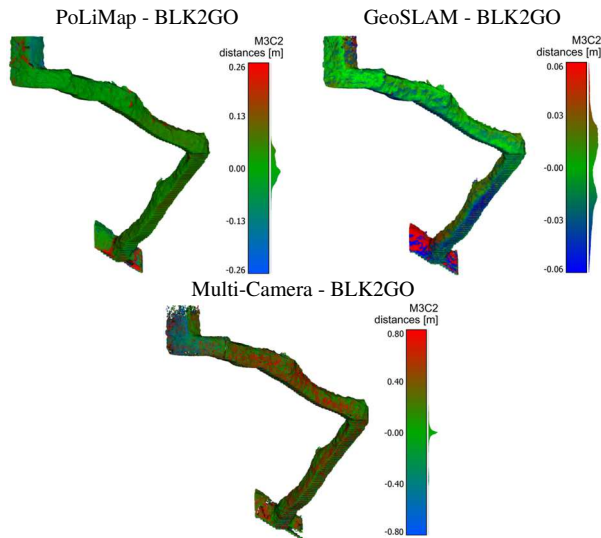


Figure 6. M3C2 comparison of point clouds from PoLiMap, GeoSLAM and ANT3D with respect to the BLK2GO for the underground case.

For the forest test site, the smallest M3C2 values occur on the ground and tree trunks. Larger differences are found in tree crowns due to the difficulty in mapping leaf objects and possible dynamics. This park area of approximately 60 x 40 m has been densely mapped with multiple, successfully recognized loop closures and repeated parts of the trajectory. No shadows or double object errors in the point cloud have been observed, despite this being a common issue with processing similar trajectories. Final standard deviation of the M3C2 distances to the reference BLK2GO data reached 13.8 cm, mostly due to the tree crowns. Using a robust error metric such as median absolute deviation, the obtained error was equal to 1.2 cm.

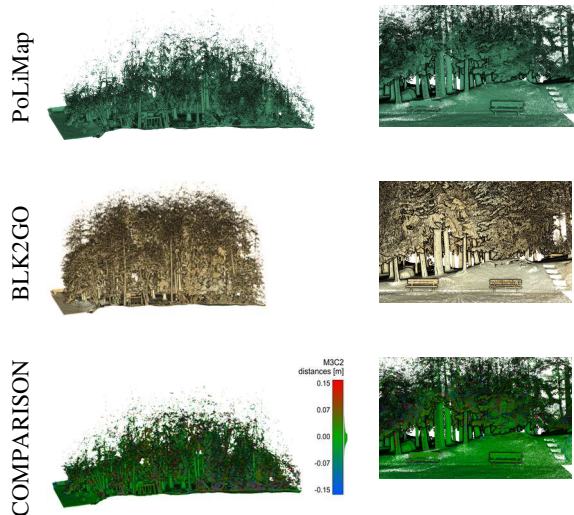


Figure 7. M3C2 comparison of point clouds from PoLiMap and BLK2GO for the forest case.

The quality assessment in the form of completeness and accuracy estimation is provided by Figure 8. Together with previous accuracy analysis, it allows to draw final conclusions from the evaluation of proposed system. Summarizing the achieved errors, it can be seen that the investigated PoLiMap system is well-suited

for mapping both indoor and outdoor environments. Urban spaces were reconstructed with mapping errors not exceeding 5 cm for 95% of points and completeness of above 90% for 10 cm threshold (Figure 8a). For underground environment, the reconstruction accuracy and the mapping completeness of Livox point cloud were similar to results of GeoSLAM. Both methods performed fantastically, approaching close to 100% metrics for distance thresholds of 5-6 cm (Figure 8b). The case study of tree and forest were also mapped with correct topology and a reasonable accuracy, although visibly degraded in foliage of the plants. While the accuracy metric reached 90% for 10 cm and 5 cm thresholds respectively, the completeness plateaued earlier, barely exceeding 80% in both cases for the highest considered threshold of 20 cm (Figures 8c and 8d). Moreover, as seen in Table 3, in almost all analysed cases median absolute deviation of comparisons to reference data was below 2.5 cm (besides foliage-rich single tree example). Considering that the measurement accuracy of a single point of the Livox scanner is 2 cm, the obtained accuracy values can be considered satisfactory and effective in the tested scenarios.

Mapping error [mm]	WUST campus	Underground				Tree		Forest
		PoLi-Map	Geo-SLAM	ANT 3D	ANT3D (without vertical shaft)	All points	Trunk	
Mean	1	-1	0	-12	11	1	5	1
Median	0	-1	3	4	4	0	0	0
Standard deviation	61	38	36	152	89	236	55	136
Median absolute deviation	10	24	18	29	21	62	7	11
95th percentile	71	65	52	362	160	53	90	91

Table 3. Mapping error values for the applied LiDAR SLAM algorithm.

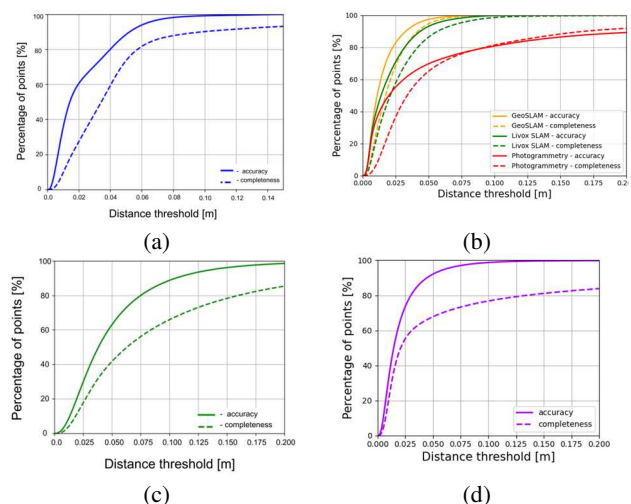


Figure 8. Accuracy and completeness curves for the proposed MMT system in all study sites: (a) WUST campus, (b) underground, (c) tree and (d) forest.

5.1 Ablation study

An ablation study is performed to evaluate whether the gimbal stabilization is bringing benefit to the final SLAM-based 3D point clouds.

Therefore additional measurements were taken in two scenarios: with and without the gimbal. The PoLiMap system was mounted on a vehicle which followed the same route two times. The 3D data captured in both scenarios were examined extracting various fragments from the data, visually comparing and calculating the root mean square error (RMSE) of fitting geometric primitives to point cloud subsets, representing several clearly distinguishable objects (tree trunks, flat elements of a facade). A set of the cross-sections is shown in Figure 9. It is noticeable that the noise level is slightly lower in the point clouds acquired with the scanner coupled to the gimbal, which proves that the device has successfully fulfilled its main function. In addition, RMSE were calculated using the fitted circle or plane and point clouds obtained with and without the stabilization device. The results in Table 4 show that smaller values are consistently observed in all cases where the gimbal was used.

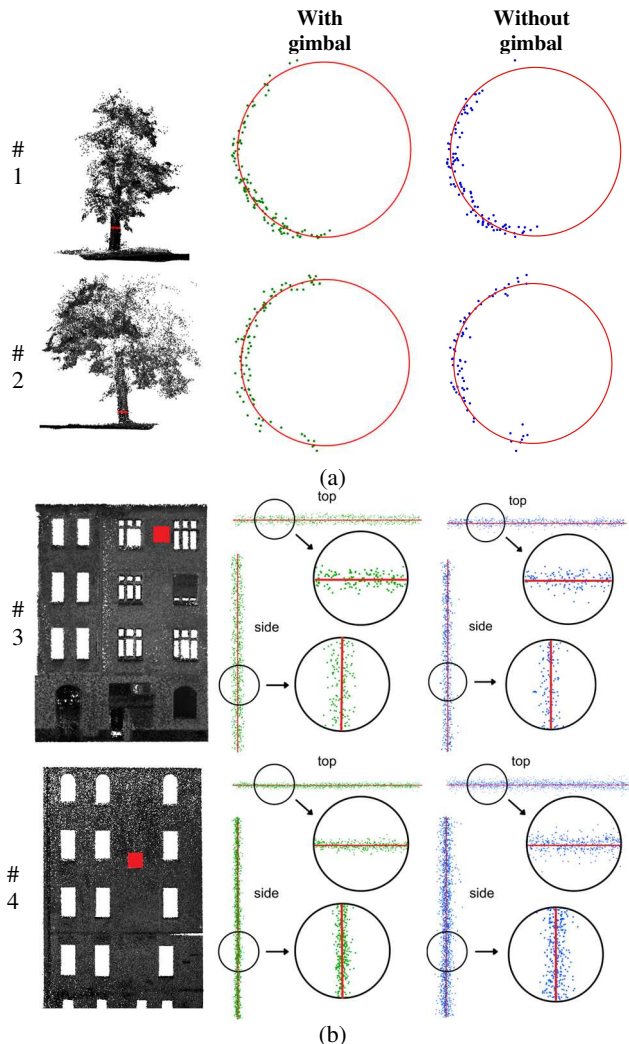


Figure 9. Examples of point cloud cross sections: trees with fitted trunk circles (a) and building walls with fitted planes (b).

Object	With gimbal	Without gimbal
#1	15	19
#2	17	20
#3	14	15
#4	8	16

Table 4. The value of the RMSE [in mm] between the fitted circle/plane and the point cloud.

Moreover, within the ablation study, we decided to quantify the difference in IMU noise levels using Power Spectral Density (PSD) analysis, which is one of the common metrics for this purpose and allows comparison of different signals in terms of their energy (Nirmal et al., 2016). PSDs were calculated using Welch's method (Welch, 1967). Resulting plots for accelerometer and gyroscope data are presented in Figures 10 and 11. Mean noise densities are compiled in Table 5. All signals from unstabilized scanner case exhibit clearly higher energy levels, especially considering higher frequencies. While the difference in mean noise values for the accelerometer varies from 50% to 100% of higher noise for the scenario without gimbal, the increase in the gyroscope mean noise density reaches over 600%. Since IMU measurements quality degradation can influence both short-term trajectory estimation and correction of point cloud distortion caused by the sensor motion, the use of a stabilization solution in conditions with possible external sources of vibrations or shaking (vehicle moving on an uneven ground, heavy machinery, etc.) can clearly contribute to improving accuracy, precision and stability of the mobile mapping system.

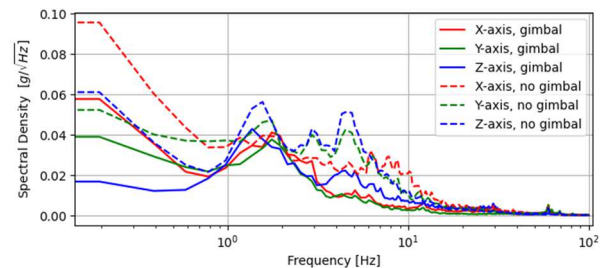


Figure 10. Power Spectral Density of the acceleration measurements in the ablation study: with gimbal (solid lines) and without gimbal (dashed lines). Frequency in a log scale.

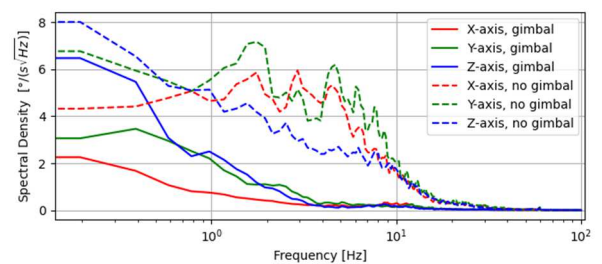


Figure 11. Power Spectral Density of the gyroscopic measurements in the ablation study: with gimbal (solid lines) and without gimbal (dashed lines). Frequency in a log scale.

Data	Axis	Mean noise density	
		Linear acceleration [$\frac{g}{\sqrt{Hz}}$]	Angular velocity [$\frac{^\circ}{s\sqrt{Hz}}$]
With gimbal	X	0.0027	0.07
	Y	0.0022	0.10
	Z	0.0031	0.11
Without gimbal	X	0.0050	0.50
	Y	0.0044	0.60
	Z	0.0045	0.42

Table 5. Mean noise densities in the ablation study obtained with PSD analysis.

6. CONCLUSIONS

The research conducted in this article presents an evaluation of the proposed PoLiMap system in different environments (urban, natural and underground). The developed low-cost MMT solution consists of a Livox Avia LiDAR sensor and a gimbal for stabilization purposes. The acquired data for the various scenarios were processed using an improved SLAM algorithm and then compared with reference data from terrestrial laser scanning and other high-quality mobile mapping systems. The effectiveness of the stabilization tool was also proved by comparing quality of raw IMU and resulting 3D data collected with and without its use.

The comprehensive evaluation of the derived 3D data in the selected use cases shows how well the proposed system can perform in different conditions. The statistics obtained from the comparison with ground truth data highlight the potential and limitations of the system for accuracy and completeness when mapping a specific environment. In all use cases the obtained metrics show satisfactory performance of the system, with great results of mapping man-made structures and reasonable results of reconstructing geometry of natural, more dynamic objects.

Worth considering how the proposed MMT portable system can be applied in practice: industrial engineering, architecture or environmental monitoring. Prospects for future advances in PoLiMap system may include a comparative analysis between a configuration utilising a sensor affixed to a handheld gimbal and an alternative setup including portable, mobile scanning devices integrated into a backpack, widely used in case-studies. Even lower costs and high customization possibilities could facilitate easy adoption of the proposed system in different industries.

ACKNOWLEDGEMENTS

This work has been partly supported by the EIT-RM project VOT3D - Ventilation Optimizing Technology based on 3D scanning (<https://vot-3d.com>).

REFERENCES

Akpınar, B., 2021: Performance of different SLAM algorithms for indoor and outdoor mapping applications. *Applied System Innovation*, 4(4), 101.

Ali, I., Durmush, A., Suominen, O., Yli-Hietanen, J., Peltonen, S., Collin, J., Gotchev, A., 2020: FinnForest dataset: A forest landscape for visual SLAM. *Robotics and Autonomous Systems*, 132, 103610.

Bienert, A., Georgi, L., Kunz, M., Maas, H.-G., Von Oheimb, G., 2018: Comparison and Combination of Mobile and Terrestrial Laser Scanning for Natural Forest Inventories. *Forests*, 9, 395.

Cheng, J., Zhang, L., Chen, Q., Hu, X., Cai, J., 2022: A review of visual SLAM methods for autonomous driving vehicles. *Engineering Applications of Artificial Intelligence*, 114, 104992.

Debeunne, C., Vivet, D., 2020: A Review of Visual-LiDAR Fusion based Simultaneous Localization and Mapping. *Sensors*, 20(7).

Dellaert, F., GTSAM Contributors. Borglab/GTSAM. 4.2a8, Georgia Tech Borg Lab, 2022.

Di Stefano, F., Torresani, A., Farella, E. M., Pierdicca, R., Menna, F., Remondino, F., 2021: 3D Surveying of Underground Built Heritage: Opportunities and Challenges of Mobile Technologies. *Sustainability*, 13(23), 13289.

Elhashash, M., Albanwan, H., Qin, R., 2022: A Review of Mobile Mapping Systems: From Sensors to Applications. *Sensors*, 22(11), 4262.

Farella, E. M., 2016: 3D mapping of underground environments with a hand-held laser scanner. *Bollettino della società italiana di fotogrammetria e topografia*, (2), 1–10.

Fasiolo, D. T., Scalera, L., Maset, E., 2023: Comparing LiDAR and IMU-based SLAM approaches for 3D robotic mapping. *Robotica*, 1-17.

Gliira, P., Weidinger, C., Kadiofsky, T., Pointner, W., Olsbock, K., Zinner, C., Doostdar, M., 2022: 3D mobile mapping of the environment using imaging radar sensors. *2022 IEEE Radar Conference (RadarConf22)*, IEEE.

He, X., Gao, W., Sheng, C., Zhang, Z., Pan, S., Duan, L., Zhang, H., Lu, X., 2022: LiDAR-Visual-Inertial Odometry Based on Optimized Visual Point-Line Features. *Remote Sensing*, 14(3).

Hyypä, E., Yu, X., Kaartinen, H., Hakala, T., Kukko, A., Vastaranta, M., Hyypä, J., 2020: Comparison of Backpack, Handheld, Under-Canopy UAV, and Above-Canopy UAV Laser Scanning for Field Reference Data Collection in Boreal Forests. *Remote Sensing*, 12(20).

Ismail, H., Roy, R., Sheu, L.J., Chieng, W. H., Tang, L. C., 2022: Exploration-Based SLAM (e-SLAM) for the Indoor Mobile Robot Using Lidar. *Sensors*, 22(4).

Janus, J., Ostrogórski, P., 2022: Underground Mine Tunnel Modelling Using Laser Scan Data in Relation to Manual Geometry Measurements. *Energies*, 15(7), 2537.

Kim, G., Yun, S., Kim, J., Kim, A., 2022a: SC-LiDAR-SLAM: A Front-end Agnostic Versatile LiDAR SLAM System. *Proc. Int. Conference on Electronics, Information and Communication (ICEIC)*, 1-6.

Kim, G., Choi, S., Kim, A., 2022b: Scan Context++: Structural Place Recognition Robust to Rotation and Lateral Variations in Urban Environments. *IEEE Transactions on Robotics*, 38(3), 1856-1874.

Knapitsch, A., Park, J., Zhou, Q. Y., Koltun, V., 2017: Tanks and temples: Benchmarking large-scale scene reconstruction. *ACM Transactions on Graphics (ToG)*, 36(4), 1-13.

- Koide, K., Yokozuka, M., Oishi, S., Banno, A., 2021: Voxelized GICP for fast and accurate 3D point cloud registration. *IEEE International Conference on Robotics and Automation (ICRA)*, 11054-11059.
- Kolhatkar, C., Wagle, K., 2020: Review of SLAM algorithms for indoor mobile robot with LIDAR and RGB-d camera technology. *Lecture Notes in Electrical Engineering, Springer Singapore*, 397–409.
- Lague, D., Brodu, N., Leroux, J., 2013: Accurate 3D comparison of complex topography with terrestrial laser scanner: Application to the Rangitikei canyon (N-Z). *ISPRS Journal of Photogrammetry and Remote Sensing*, 82, 10-26.
- Livox Avia Quick Start Guide v1.4, 2021. Brochure. Accessed 25.09.2023:
https://terra-1-g.djicdn.com/65c028cd298f4669a7f0e40e50ba1131/Download/Avia/Livox%20Avia_Quick%20Start%20Guide_V1.4.pdf
- Menna, F., Battisti, R., Nocerino, E., Remondino, F., 2023: FROG: a portable underwater mobile mapping system. *Int. Arch. Photogramm. Remote Sens. Spatial Inf. Sci.*, XLVIII-1/W1-2023, 295–302
- Nirmal K., Sreejith A. G., Mathew, J., Sarpotdar, M., Suresh, A., Prakash, A., Safonova, M., Murthy, J., 2016: Noise modeling and analysis of an IMU-based attitude sensor: improvement of performance by filtering and sensor fusion, *Proc. SPIE 9912*, 99126W.
- Nocerino, E., Menna, F., Remondino, F., Toschi, I., Rodríguez-González, P., 2017: Investigation of indoor and outdoor performance of two portable mobile mapping systems. *SPIE Proc.* 10332.
- Pan, D., Shao, J., Zhang, S., Zhang, S., Chang, B., Xiong, H., Zhang, W. 2023: SLAM-based Forest Plot Mapping by Integrating IMU and Self-calibrated Dual 3D Laser Scanners. *IEEE Transactions on Geoscience and Remote Sensing*.
- Perfetti, L., Elalaily, A., Fassi, F., 2022: Portable Multi-Camera System: from Fast Tunnel Mapping to Semi-Automatic Space Decomposition and Cross-Section Extraction. *International Archives of the Photogrammetry, Remote Sensing and Spatial Information Sciences*, 43, 259-266.
- Perfetti, L. and Fassi, F., 2022: Handheld fisheye multicamera system: surveying meandering architectonic spaces in open-loop mode – accuracy assessment. *Int. Arch. Photogramm. Remote Sens. Spatial Inf. Sci.*, XLVI-2/W1-2022, 435–442.
- Pierzchała, M., Giguère, P., Astrup, R., 2018: Mapping forests using an unmanned ground vehicle with 3D LiDAR and graphSLAM. *Computers and Electronics in Agriculture*, 145, pp. 217- 225.
- Qian, C., Liu, H., Tang, J., Chen, Y., Kaartinen, H., Kukko, A., Zhu, L., Liang, X., Chen, L., Hyypä, J., 2016: An Integrated GNSS/INS/LiDAR-SLAM Positioning Method for Highly Accurate Forest Stem Mapping. *Remote Sensing*, 9(1), 3.
- Rouveure, R., Faure, P., Monod, M. O., 2021: Terrestrial mobile mapping based on a microwave radar sensor. Application to the localization of mobile robots. *ISPRS Annals of the Photogrammetry, Remote Sensing and Spatial Information Sciences*, V-1-2021, 73–80.
- Sesmero, C. P., Lorente, S. V., Castro, M. D., 2021: Graph SLAM Built over Point Clouds Matching for Robot Localization in Tunnels. *Sensors*, 21(16), 5340.
- Shao, J., Zhang, W., Mellado, N., Wang, N., Jin, S., Cai, S., Luo, L., Lejemble, T., Yan, G., 2020: SLAM-aided forest plot mapping combining terrestrial and mobile laser scanning. *ISPRS Journal of Photogrammetry and Remote Sensing*, 163, 214-230.
- Singandhupe, A., La, H. M., 2019: A review of SLAM techniques and security in autonomous driving. *2019 Third IEEE International Conference on Robotic Computing (IRC)*, IEEE.
- Sonugür, G., 2023: A Review of quadrotor UAV: Control and SLAM methodologies ranging from conventional to innovative approaches. *Robotics and Autonomous Systems*, 161, 104342.
- Tanduo, B., Martino, A., Balletti, C., & Guerra, F., 2022: New Tools for Urban Analysis: A SLAM-Based Research in Venice. *Remote Sensing*, 14(17), 4325.
- Torresani, A., Menna, F., Battisti, R., Remondino, F., 2021: A V-SLAM Guided and Portable System for Photogrammetric Applications. *Remote Sensing*, 13(12), 2351.
- Trybała, P., Kasza, D., Wajs, J., Remondino, F., 2023a: Comparison of low-cost handheld LiDAR-based SLAM systems for mapping underground tunnels. *The International Archives of the Photogrammetry, Remote Sensing and Spatial Information Sciences*, XLVIII-1/W1-2023, 517–524.
- Trybała, P., Szrek, J., Remondino, F., Kujawa, P., Wodecki, J., Balchowski, J., Zimroz, R., 2023b: MIN3D dataset: Multi-sensor 3D mapping with an unmanned ground vehicle. *PGF – Journal of Photogrammetry, Remote Sensing and Geoinformation Science*, in press.
- Wang, M., Long, X., Chang, P., Padlr, T., 2018: Autonomous robot navigation with rich information mapping in nuclear storage environments. *2018 IEEE International Symposium on Safety, Security, and Rescue Robotics (SSRR)*, IEEE, 1-6.
- Welch, P., 1967: The use of the fast Fourier transform for the estimation of power spectra: A method based on time averaging over short, modified periodograms, *IEEE Trans. Audio Electroacoust.*, 15, 70-73.
- Wróblewski, A., Trybała, P., Banasiewicz, A., Zawisłak, M., Walerysiak, N., Wodecki, J., 2023: Possibilities of 3D laser scanning data utilization for numerical analysis of airflow in mining excavations. *IOP Conference Series: Earth and Environmental Science*, 1189(1), 012009.